IL NUOVO CIMENTO Vol. 35 C, N. 5 Settembre-Ottobre 2012
DOI 10.1393/ncc/i2012-11319-1

Communications: SIF Congress 2011

Study of magnetic domain wall trapping forces on superparamagnetic beads for on chip biological manipulation

A. Torti(*)

L-NESS and Cnism, Dipartimento di Fisica, Politecnico di Milano via Anzani 42, 22100 Como, Italy

ricevuto il 16 Febbraio 2012; revisionato il 12 Aprile 2012; approvato il 10 Giugno 2012

Summary. — The manipulation of biological molecules and single cells on a surface is of fundamental importance for the development of novel magnetic lab-on-chip tools for biological and medical applications. Geometrically constrained magnetic domain walls (DWs) in permalloy nano- and micro-conduits can be manipulated precisely by applying weak external magnetic fields. The inhomogeneous magnetic stray field generated by a DW can capture magnetic beads in solution. The use of the highly controllable motion of these DWs allows the handling of functionalized magnetic particle and labeled single yeast cells within a microfluidics cell. In this paper we study both via simulations and experimentally the DWs micromagnetic configurations and the force exerted on a superparamagnetic bead. These results show the versatility of domain wall conduits in manipulating different biological entities in lab-on-chip devices. Networks of conduits containing bifurcations, curved portions and DW-AMR sensors can enlarge the range of practical applications.

PACS 75.78.Cd – Micromagnetic simulations.
PACS 75.60.Ch – Domain walls and domain structure.
PACS 87.85.Qr – Nanotechnologies - applications in biology.

1. – Introduction

Methods for manipulating proteins, bacteria and living cells in lab-on-chip devices can open new possibilities in biology, medicine and biotechnology. These techniques ultimately lead to the development of reproducible, automated and efficient systems to be employed in research laboratories as well in industrial and clinical applications. In this context, methods based on the remote manipulation of magnetic beads functionalized

(*) E-mail: andrea.torti@mail.polimi.it

with proteins, genes or bound to cells, via external or local magnetic fields, are receiving great attention essentially because: i) magnetic fields are not screened by biological matter and culture media (at variance with, *e.g.*, dielectrophoretic trapping, which requires instead the use of non-conductive media) so that manipulation is possible in any chemical environment; ii) magnetic manipulation does not involve relevant energy dissipation, which could eventually damage biological structure, which is the case for optical tweezers [1]. Trapping biological entities like cells on a patterned substrate or scaffold according to a precise geometry is of major importance for various applications such as cell cultivation, interaction, production and regeneration of tissues, investigation of cell-surface aggregation and of the dynamics of cellular processes [2]. Many different techniques have been developed to accomplish this task, including passive techniques relying on cell-substrate chemical interactions and active techniques, where cells are attracted towards the desired site, as in the case of magnetic forces on particles bound to cells, originating from localized stray fields emanated by magnetic structures [3,4]. Traps based on permalloy microstructures [5] or pillars of magnetic materials [6] have been recently proposed to capture cells to form an array, in order to allow for studies on a large population of individual cells in a single experiment. We recently demonstrated a novel method, based on the utilization of controlled injection and propagation of individual DWs in magnetic nano- and micro-wires, for on-chip manipulation of single magnetic particles functionalized with proteins [7] or cell decorated by many beads [8]. In this framework the study of the micromagnetic mechanisms responsible for trapping force is interesting because by engineering the geometry of the structure we are able to tailor the trapping forces thus giving different functionalities to the final device. The trapping force arises from two different kinds of domain walls, transverse and vortex-state, which can be created in magnetic wires having different lateral size. As a major output, the use of zigzag wires having lateral size of few microns is shown to be particularly convenient for cells applications.

2. – Experimental

2˙1. *Chip fabrication.* – Series of corners employed in this work were made of permalloy ($Ni_{80}Fe_{20}$) zigzag wires with thickness $t = 25\,\text{nm}$ and witdh $w_n = 200\,\text{nm}$ for nano-corners or $w_m = 2\,\mu\text{m}$ for micro-corners. The nanostructures have been fabricated on top of SiO_2/Si substrate by e-beam lithography followed by lift-off, as previously described [7,9]. Microstructures have been instead patterned by optical lithography. Figure 1 shows the two chips surfaces containing the lithographed arrays of nano- and micro-corners.

Both structures have been covered by a protective SiO_2 coating layer of thickness $t_c = 50\,\text{nm}$ in order to protect the magnetic wires and to prevent non-magnetic and non-selective binding between beads and the substrate. For the experimental evaluation of the force acting on beads trapped by nano-sized or micro-sized corners, a micro-channel (width $= 600\,\mu\text{m}$, height $= 65\,\mu\text{m}$) was fabricated by soft lithography, casting polydimethylsiloxane (PDMS) on an SU-8 (Microchemicals, Germany) master, and finally bonded on the chip with magnetic conduits by O_2 plasma treatment. This channel was then connected an external syringe pump to precisely define the liquid velocity by the application of a given liquid flow rate.

2˙2. *Micromagnetic simulations.* – Since the functionalities of magnetic DW conduits are strongly related to the geometry of the nanostrips, micromagnetic simulations were performed in order to study the magnetization equilibrium states and the magnetic force

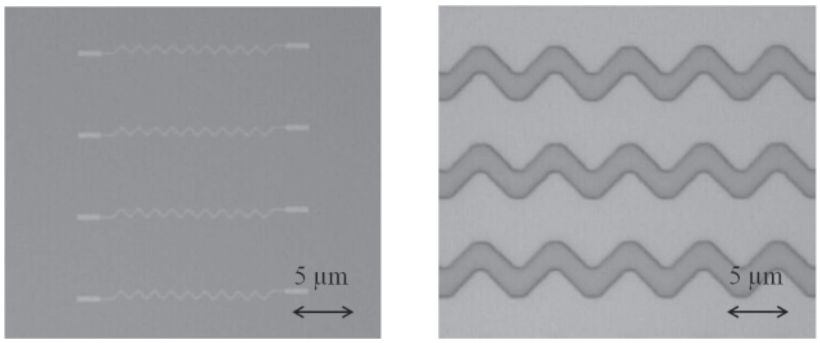

Fig. 1. – Optical microscope images of zigzag conduits, 25 nm thick, made of permalloy a) nano-corners with a width = 200 nm, length of the corner segment = 2 μm; b) micro-corners with a width of = 2 μm, length of the segment = 6 μm.

generated. The public OOMMF (Object Oriented Micro Magnetic Framework) platform [10] has been used with the following parameters for permalloy: saturation magnetization $M_s = 800 \cdot 10^3\,\mathrm{A\,m^{-1}}$, exchange stiffness constant $A = 1.3 \cdot 10^{-11}\,\mathrm{J\,m^{-1}}$, damping coefficient = 0.5, no magnetocrystalline anisotropy has been considered. The damping coefficient is high, compared to the experimental one; this leads to a faster computation of the equilibrium state, that is what we are interested in, but lose accuracy in describing the transient behavior. We used two quasi-cubic cells of 10 nm side and 12.5 nm high and of 20 nm side and 25 nm high for the simulation of nanocorners and microcorners respectively; both greater than the exchange length of 5.2 nm given by $\lambda_{ex} = \sqrt{\frac{2A}{\mu_0 M_s^2}}$ but still the smallest ones compatible with the computational time. For the simulation we used parameters related to standard commercial Spherotec 1 μm diameter beads; in detail a magnetic susceptibility χ of 0.39 has been chosen.

2˙3. *Magnetic attractive force measurements.* – The force from DWs on trapped magnetic beads was measured by comparing the attractive magnetic force with the hydrodynamic drag force which tends to detach the bead from the DW. The chips with several arrays of magnetic nano- or micro-corners were washed inside the microfluidic channel with a solution of 1% v/v Triton X-100 and 1%w/v BSA in PBS, in order to block the chip surface. For both nano- and micro-corners DWs were created at every corner to maximize the number of trapping sites by applying an in-plane external magnetic field of 50 mT, perpendicular to the long axis of the zigzag conduit. A suspension containing 10^6 particle per μl was injected in the fluidic channel at a very low flow rate. Once a population of beads has been attracted by the magnetic corners, the liquid flow rate was constantly increased while acquiring a video via a camera mounted on an optical microscope (Nikon Eclipse FN1 with 60× water immersion objective). The number of events of trapping and detaching of beads from the corners was counted through a video analysis using the camera software (Nis Element BR, US). The effective liquid velocity was estimated from the average speed of magnetic beads moving freely in the solution just above the chip surface, within 2 μm, that is the depth of focus of the microscope

objective. The hydrodynamic drag force was estimated as

$$F_d = 3\pi\eta d\nu K, \tag{1}$$

where η is the viscosity of the surrounding fluid ($= 10^3$ Pa s for water), d is the diameter of the spherical bead, ν is the relative velocity between particles and the fluid. K is the drag coefficient, it accounts for the interaction of particles close to a solid wall (the surface, in our case). For a particle having a diameter of 1 μm, we estimated a value of $K = 3$ using the formula derived in ref. [11]. We also assumed that the particle is not rolling, which is the case of a particle just after the detaching event.

3. – Results and discussion

As mentioned above, domain walls in magnetic nanowires have been demonstrated to be suitable for manipulation of individual protein-coated magnetic beads ranging from 500 nm to 3 μm of diameter in suspension [7]. To apply such technology to cells trapping and transport it is necessary to tailor the device size in order to transport much larger entities, as cells labelled with magnetic beads (5–15 μm). The estimation of the trapping force arising from magnetic corners of different dimensions was carried out both theoretically, via micromagnetic simulation, and experimentally, by using the setup described in experimental section.

3˙1. *Domain wall configuration and relative force calculations.* – In permalloy magnetic structures like those considered in the present work, *i.e.*, thin stripes with various geometrical shapes, different types of DWs are observed essentially depending on the ratio between the thickness t and the width w. According to the DW "phase diagram" [12], for 25 nm $< t <$ 40 nm, transverse DWs are created in magnetic wires with $w = 200$ nm, while vortex DWs enucleate in structures with $w = 2\,\mu$m. The comparison between the two cases is interesting because transverse DWs typically produce a strong highly localized stray field, while vortex DWs are expected to give rise to a less intense stray field because of tendency to close the magnetic flux. However we demonstrate that in micron-sized corners the vortex state generates an irregular stray field which exerts forces on superparamagnetic bead as high as those by transverse DW but with a much larger spatial extension. This fact makes this peculiar type of DW more suitable for capturing extended bodies like a cell labelled with many magnetic particles. Once we got the equilibrium spin structure of the corners, we simulate the magnetic stray field $\mathbf{H}_{\mathrm{DW}}$ generated by such micromagnetic configuration. The magnetic vector field $\mathbf{H}_{\mathrm{DW}}$ is then processed in a *Matlab* script. The bead magnetization $\mathbf{m}_b$ is assumed homogeneous throughout its volume and it is related to the magnetic field by its experimental susceptibility χ:

$$\mathbf{m}_b = \chi \cdot \mathbf{H}_{\mathrm{DW}}. \tag{2}$$

The magnetic energy of a bead above a DW is thus calculated by integrating the energy density $-\mathbf{m}_b \cdot \mathbf{B}_{\mathrm{DW}}$ over the particle volume and considering $\mathbf{B}_{\mathrm{DW}} = \mu_0 \mathbf{H}_{\mathrm{DW}}$:

$$E_b = -\mu_0 \chi \int_{V_b} \mathbf{H}_{\mathrm{DW}} \cdot \mathbf{H}_{\mathrm{DW}}\, \mathrm{d}V. \tag{3}$$

Figure 2(a,b) shows the magnetic potential landscape for beads having a diameter $d_b =$ 1 μm on a plane at a distance $z = d_b/2 + t_c = 550$ nm from the transverse and vortex

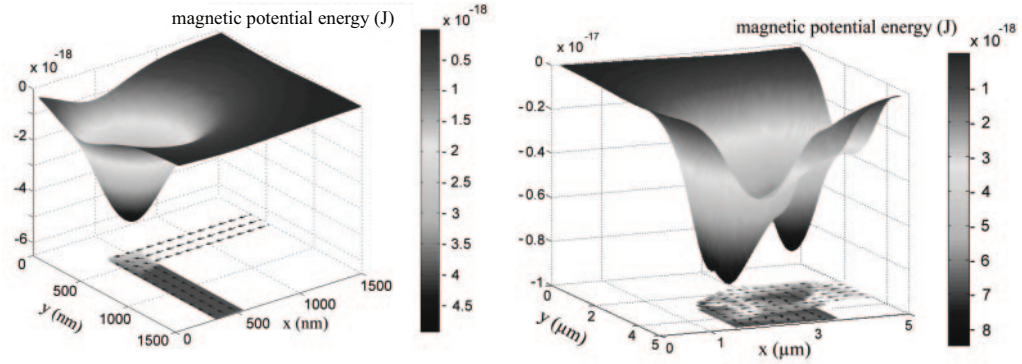

(a) (b)

Fig. 2. – Micromagnetically computed domain wall structure in a) 200 nm wide ×25 nm thick and b) 2 μm wide ×25 nm thick permalloy corner. Above each micromagnetic configuration, the magnetic potential energy is shown for a superparamagnetic particle with a diameter of 1 μm. The distance between the bottom of the particle and the substrate surface is 50 nm. Magnetic susceptibility of the simulated bead χ is 0.39.

DW, respectively. The micromagnetic spin structure, depicted below each potential, is the result of OOMMF simulations of permalloy corners (25 nm thick and 200 nm or 2 μm wide) after the application and removal of a 50 mT external magnetic field along the corner bisector. The potential landscape generated by the nano-corner has a single, nearly parabolic well, confined to the transverse DW. By contrast, the stray field of the micro-corner yields an irregular multi-wells potential positioned at the external edge of the corner.

The force vector field and its 3 Cartesian components are then simply computed from the gradient of the magnetic potential.

$$\mathbf{F} = -\nabla E_b, \tag{4}$$

$$F_x = -\frac{\partial E_b}{\partial x}, \qquad F_y = -\frac{\partial E_b}{\partial y}, \qquad F_z = -\frac{\partial E_b}{\partial z}.$$

In fig. 3 the contour plots of the force along z (the axis normal to the surface) derived from the previous calculated magnetic potential are illustrated. Dark areas correspond to the highest intensity of the force. The negative value of the force simply means that its direction points towards the surface (attractive force). The integration over the bead volume avoids the point dipole assumption which is a rough approximation especially when for a 1 μm bead the diameter is larger than the corner width. The maximum values of the transverse forces (*i.e.* along z) in the two cases are 45.2 pN and 62.7 pN, generated by the nano-sized and micro-sized corner, respectively.

The peak value of the vortex DW is comparable to that one of the transverse DW but the spatial profile is quite different. For nano-corner the force is concentrated in an area with a diameter of 300 nm, whereas in the micro-corner the vortex DW creates different attraction poles spread over a quasi-elliptical area of 4 μm × 2 μm. From this analysis it clearly results that vortex DWs enucleated in micro-corners are more suitable for manipulating comparatively larger biological entities, like cells or bacteria.

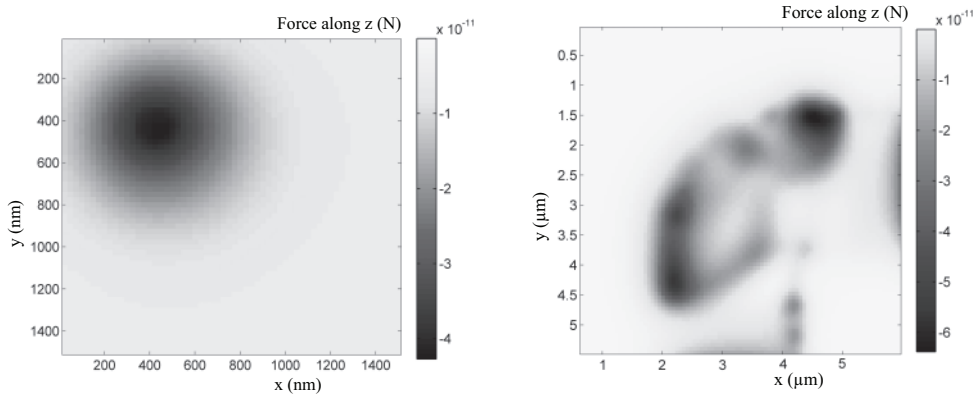

(a) (b)

Fig. 3. – Contour plots of the calculated force on a Spherotec ($\chi = 0.39$, 1 μm diameter) magnetic bead *vs.* the bead center position when the bead is moving on a plane at a distance of 550 nm from the surface.

3˙2. *Experimental evaluation of the trapping forces*. – To validate the calculated trapping forces, we measured the liquid flow rate at which the liquid drag force on the bead overcomes the DW trapping force. The procedure described in the experimental section was applied varying the liquid flow rate from 5 μl min^{-1} to 50 μl min^{-1} in the microchannel. The velocity of the solution was estimated both analitically through the flow rate and experimentally by measuring the average speed of beads moving freely just above the chip surface. Results are summarized in fig. 4. The net percentage of detaching events (net events), *i.e.* the number of detaching events lowered by the number of sticking events recorded during the very same observation time (1 min) and normalized to the initial number of trapped magnetic beads, is shown as a function of the liquid flow rate. When increasing the flux, the corresponding increase of the liquid speed produces

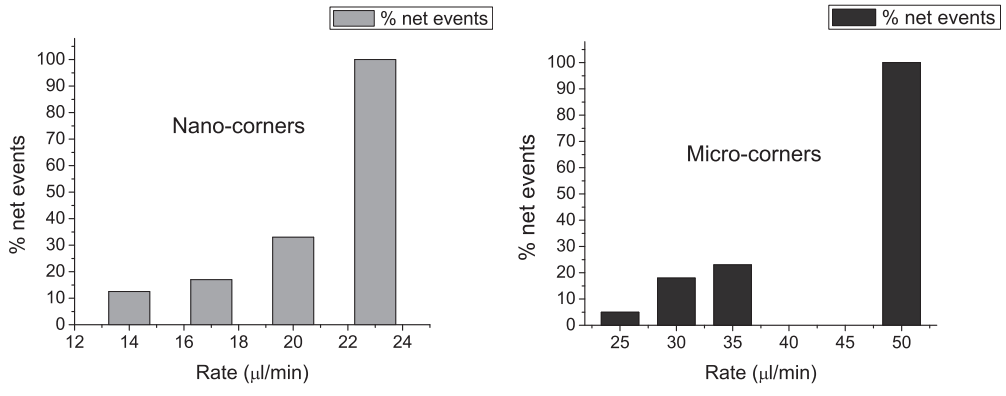

(a) (b)

Fig. 4. – Histograms of the net number of detaching events percentage (% net events) *vs.* the liquid flow rate established via the syringe pumps for nano-corners (a) and micro-corners (b).

a higher hydrodynamic force on the magnetic beads, eventually leading to a complete detachment of trapped beads (net events = 100%) which represents the end condition of our experiments. To take into account the statistical distribution of detaching events the fluid velocity v to be inserted in eq. (1) has been evaluated taking the average of the velocities related to the flow rate reported in fig. 4 weighted by the net number of detaching events. This gives $v = (433 \pm 133)\,\mu$m/s for nano-sized corners and $(1131 \pm 307)\,\mu$m/s for micron-sized corners, where the uncertainties indicate one standard deviation.

The corresponding measured trapping forces are (16 ± 5) pN and (43 ± 5) pN for nano-corners and micro-corners, respectively. The higher average trapping force measured for vortex DW in micro-corners confirms the prediction of the micromagnetic calculations. As shown by the experiments, different magnitudes and distributions of the trapping force arise from different micromagnetic configuration. In particular the distribution of the force in micro-corner results more suitable for achieving efficient cells manipulation, with single entity precision.

4. – Conclusion

We have presented a study on magnetic trapping forces generated by confined domain walls in permalloy micro- and nano-structures. On-chip proteins or cell manipulation based on remotely controlled DW motion has great potential for cell investigation as well as for diagnostic and drug discovery applications. The *matlab* post processing of the OOMMF simulated stray field allows for taking into account the bead volume size w.r.t. the spatial extension of the DW stray field. In this way every factor contributing to the net value of the force is better understood. We have demonstrated that permalloy nano-corners can be appropriate to trap and manipulate single superparamagnetic particles with a diameter up to $3\,\mu$m, functionalized with proteins or biological molecules. If the objects of manipulation are bigger entities, like single cells decorated with many particles, then permalloy micro-cornes are more suitable since they exert a more intense and spatial expanded force field on superparamagnetic particles in suspension above them. These magnetic traps can be easily integrated with platforms for the detection of magnetic labels, such as DW-AMR sensors [13] or TMR sensors [14], thus achieving a direct electrical transduction of the signals related to individual biological entities positions.

* * *

The author thanks V. Mondiali, M. Donolato, M. Leone and R. Bertacco for assistance during the experiments and useful discussions. This work was supported by Fondazione Cariplo *via* the project SpinBioMed (grant No. 2008.2330) and NanoMed (grant No.2010.214) and by funding from the Basque Government through the ETORGAI Program (Project No. ER-2010/00032 and Program No. PI2009-17).

REFERENCES

[1] Lindstrom S. and Andersson-Svahn L., *Lab Chip*, **10** (2011) 3363.
[2] Griffith L. G. and Naughton G., *Science*, **295** (2002) 1009.
[3] Tanase M., Felton E. J., Gray D. S., Hultgren A., Chen C. S. and Reich D. H., *Lab Chip*, **5** (2005) 598.

[4] Bryan M. T., Smith K. H., Real M. E., Bashir M. A., Fry P. W., Fischer P., Im M., Schrefl T., Allwood D. A. and Haycock J. W., *IEEE Magn. Lett.*, **1** (2010) 1500104.
[5] Liu W., Dechev N., Foulds I. G., Burke R., Parameswaran A. and Park E. J., *Lab Chip*, **9** (2009) 2381.
[6] Ino K., Okochi M., Konishi N., Nakatochi M., Imai R., Shikida M., Ito A. and Honda H., *Lab Chip*, **8** (2008) 134.
[7] Donolato M., Gobbi M., Vavassori P., Deryabina M., Hansen M. F., Metlushko V., Ilic B., Cantoni M., Petti D., Brivio S. and Bertacco R., *Adv. Mater*, **22** (2010) 2706.
[8] Donolato M., Torti A., Kostesha N., Deryabina M., Sogne E., Vavassori P., Hansen M. F. and Bertacco R., *Lab Chip*, **11** (2011) 2976.
[9] Donolato M., Gobbi M., Vavassori P., Leone M., Cantoni M., Metlushko V., Ilic B., Zhang M., Wang S. X. and Bertacco R., *Nanotechnology*, **20** (2009) 385501.
[10] Donahue M. J. and Porter D. G., *OOMMF User's guide version 1.0, interagency Report NISTIR 63 76*, NIST, Gaithersburg, 1999.
[11] Happel J. and Brenner H., *Low Reynolds Number Hydrodynamics* (Kluwer, Boston, MA) 1983.
[12] Laufenber M., Backes D., Bhrer W., Bedau D., Klui M., Rdiger U., Vaz C. A. F., Bland J. A. C., Heyderman L., Nolting F., Cherifi S., Locatelli A., Belkhou R., Heun S. and Bauer E., *Appl. Phys. Lett.*, **88** (2006) 05207.
[13] Vavassori P., Metlushko V., Ilic B., Gobbi M., Donolato M., Cantoni M. and Bertacco R., *Appl. Phys. Lett.*, **93** (2008) 203502.
[14] Donolato M., Sogne E., Dalslet B. T., Cantoni M., Petti D., Cao J., Cardoso F., Cardoso S. and Freitas P. P., *Appl. Phys. Lett.*, **98** (2011) 073702.